ChemPubSoc Europe

DOI: 10.1002/cssc.201500631

CHEMSUSCHEM Full Papers

Elucidating the Role of Conjugated Polyelectrolyte Interlayers for High-Efficiency Organic Photovoltaics

Kyung-Geun Lim,[a] Sung Min Park,[b] Han Young Woo,*[b] and Tae-Woo Lee*[a]

Despite the promising function of conjugated polyelectrolytes (CPEs) as an interfacial layer in organic photovoltaics (OPVs), the underlying mechanism of dipole orientation and the electrical characteristics of CPE interlayers remain unclear. Currently, the ionic functionality of CPEs (i.e., whether they are cationic or anionic) is believed to determine the interfacial dipole alignment and the resulting electron or hole extraction properties at the interface between an organic photoactive layer and a metal electrode. In this research, we find that in contrast to this common belief, the photovoltaic efficiency can be improved significantly by both cationic and anionic CPE layers regardless of the ion functionality of the CPE. This improvement occurs because the interfacial dipoles of cationic and anionic CPEs are realigned in the identical direction despite the different ionic functionality. The net dipole is determined not by the intrinsic molecular dipole of the CPE but by the ionic redistribution in the CPE layer and the resulting interfacial dipole at the intimate contact with adjacent layers. We also demonstrated that the energy level alignment and performance parameters of OPVs can be controlled systematically by the electrically poled CPE layers with the oriented interfacial dipoles; the distribution of positive and negative ions in the CPE layer was adjusted by applying an appropriate external electric field, and the energy alignment was reversible by changing the electric field direction. The anionic and cationic CPEs (PSBFP-Na and PAHFP-Br) based on the same π-conjugated backbone of fluorene-phenylene were each used as the electron extraction layer on a photoactive layer. Both anionic and cationic CPE interlayers improved the energy level alignment at the interface between the photoactive layer and the electrode and the resulting performance parameters, which thereby increased the power conversion efficiency to 8.3%.

Introduction

In organic photovoltaics (OPVs) charge extraction is critically sensitive to interfacial contact between an organic photoactive layer and the metal electrodes and can be adjusted by the insertion of various kinds of interfacial layers.[1] Conjugated polyelectrolytes (CPEs) are promising interfacial layer materials for OPVs because of advantages such as solution processability with polar solvents and energy level adjustment ability.[2–21] As a result of the ionic nature of CPEs, they are soluble in polar solvents (e.g., water, alcohol) and can be deposited underneath (or on top of) the active layer as an interfacial layer of single-junction OPVs or an interconnection layer of series-connected tandem OPVs.[19]

Although the CPE interlayer deposited underneath the metal electrode modifies the work function (WF) of the electrode and reduces the interfacial energy barrier in organic electronic devices,[3–11] the manner in which CPE generates a dipole moment at the interfaces is not yet fully understood. Although several methods use cationic CPE layers to improve the electron extraction in OPVs,[2–20] little attention has been paid to anionic CPEs for the electron extraction interlayer. Cationic CPEs, such as poly{9-[*N,N*-di(2′′-hydroxyethyl)-6′-aminohexyl]-2,7-carbazole}-*alt*-{2-hexyloxy-5-[*N,N*-di(2′′-hydroxyethyl)-6′-aminohexyloxy]-1,4-phenylene} (PCP-NOH),[2] poly{9,9-bis[3′-(*N,N*-dimethylamino)propyl]-2,7-fluorene}-*alt*-2,7-(9,9-dioctylfluorene) (PFN),[3–8] poly(fluorene-*co*-phenylene) (PFP),[12] poly{9,9-bis[6′-(*N,N,N*-trimethylammonium)hexyl]fluorene}-bromide (WPFN), poly{9,9-bis6[-(*N,N,N*-trimethylammonium)hexyl]-2,7-fluorene}-*alt*-{9,9-bis[2-(2-methoxyethoxy)ethyl]-fluorene} dibromide (WPF-oxy-F),[13–15] poly{9,9-bis[6′-(*N,N,N*-trimethylammonium)-hexyl]fluorene-*alt*-*co*-1,4-phenylene}bromide (FPQ-Br),[16–19] HT-poly[3-(60-*N,N,N*-trimethylammonium)-hexyl thiophene] (P3HTN),[20] poly[3-(6-trimethylammoniumhexyl)thiophene] (P3TMAHT),[21] and PTNBr,[22] have been used as electron extraction layers in OPVs.

The vacuum energy level (E_{vac}) at the metal–semiconductor interface could be rearranged depending on the direction of the dipole moment at interfaces that include a CPE layer. It is believed that the dipole moment generated by cationic CPEs reduces the energy offset between the LUMO level of a photoactive semiconductor and the WF of the cathode, whereas anionic CPEs increase the energy offset at the electron extraction contact because the interfacial dipole moments are in op-

[a] *K.-G. Lim, Prof. T.-W. Lee*
Department of Materials Science and Engineering
Pohang University of Science and Technology (POSTECH)
San 31 Hyoja-dong, Nam-gu, Pohang
Gyungbuk 790-784 (Republic of Korea)
E-mail: twlee@postech.ac.kr

[b] *S. M. Park, Prof. H. Y. Woo*
Department of Chemistry
Korea University
Seoul 136-713 (Republic of Korea)
E-mail: hywoo@korea.ac.kr

Supporting Information for this article is available on the WWW under http://dx.doi.org/10.1002/cssc.201500631.

posite directions.[16] PFN was used as an electron extraction layer underneath the active layer in an inverted OPV device to reduce the effective WF of indium tin oxide (ITO)[3] and it can be used on top of the active layer to improve electron extraction in a normal OPV device by forming an interface dipole.[4] However, a clear explanation of the mechanism and correlation between the device characteristics with the measured dipole moment of the CPE interlayer[4] has not been given.

In this study, we applied alcohol-/water-soluble CPEs with the opposite ionic functionality (i.e., cationic vs. anionic) as a cathode interlayer in bulk heterojunction OPV cells and demonstrated the improved photovoltaic efficiency with anionic and cationic CPE layers. We also demonstrated that the distribution of ionic groups and the resulting direction of the interfacial dipole moment at the interfaces, which include ultrathin CPE layers, can be controlled reversibly by an external electric field despite the different kinds of ionic functionality in the CPEs. We synthesized two anionic and cationic CPEs based on the same polymeric backbone, poly[9,9′-bis(4-sulfonatobutyl)-fluorene-*alt*-1,4-phenylene] disodium salt (PSBFP-Na) and poly[9,9′-bis(6′′-*N*,*N*,*N*-trimethylammoniumhexyl]fluorene-*alt*-1,4-phenylene) dibromide (PAHFP-Br). If we used the CPEs as an electron extraction layer on top of the photoactive layer, both the cationic and anionic CPE layers improved the energy level alignment at the interfacial contact with the electrode, which thereby resulted in an increased power conversion efficiency (PCE). This observation contradicts the predictions of the current model. In addition, further improvement in the PCE was achieved by applying external bias (so-called electric poling) to devices; this bias causes dipole reorientation in the ultrathin CPE interlayer to minimize the interfacial energy offset. In previous reports, the distribution of ionic groups in the CPE thin films in OPVs was estimated roughly from information about the dipole moment determined by the E_{vac} shift[16] or surface potential.[4,22] Here, we studied the mechanism for the generation and orientation of dipole moments at interfaces, which includes CPE layers. Despite the different ionic functionality and the intrinsic molecular dipole of the CPEs, we find that the interfacial dipole moment generated by anionic CPEs is nearly identical to that of cationic CPEs if the CPEs are deposited on top of the photoactive layer and the corresponding devices are poled electrically. Furthermore, to elucidate the mechanism by which ionic groups are redistributed and thereby dipoles are generated and reorientated, we used electric poling to investigate the correlation between the interfacial dipole moment and the controlled distribution of ionic groups in the CPE layer. Finally, we achieved a high PCE of 8.3% for a poly({4,8-bis[(2-ethylhexyl)oxy]benzo[1,2-b:4,5-b′]dithiophene-2,6-diyl}{3-fluoro-2-[(2-ethylhexyl)carbonyl] thieno[3,4-b]thiophenediyl}) (PTB7):[6,6]-phenyl C70-butyric acid methyl ester ($PC_{70}BM$) OPV device with either an anionic or a cationic CPE interlayer as the electron extraction layer.

Results and Discussion

We synthesized anionic and cationic CPEs PSBFP-Na and PAHFP-Br by modification of procedures reported previously.[17,18] Anionic PSBFP-Na has sulfonate moieties in its side chains, and cationic PAHFP-Br contains quaternized ammonium groups (Figure 1). We investigated the photovoltaic characteristics of poly[*N*-9′′-heptadecanyl-2,7-carbazole-*alt*-5,5-(4′,7′-di-2-thienyl-2′,1′,3′-benzothiadiazole) (PCDTBT)[23–26] and $PC_{70}BM$ OPVs with a normal device architecture of ITO/PEDOT:PSS/PCDTBT:$PC_{70}BM$/CPE interlayer/Al. To explore the impact of the CPE interlayers on the device characteristics, either PAHFP-Na or PSBFP-Br was spin-coated on top of the photoactive layer as the electron extraction layer. In contrast to conventional beliefs, both the cationic and anionic CPE layers capped with Al improved the performance parameters of OPVs compared with the Al and Ca/Al cathode without the CPE layers (Table 1). The

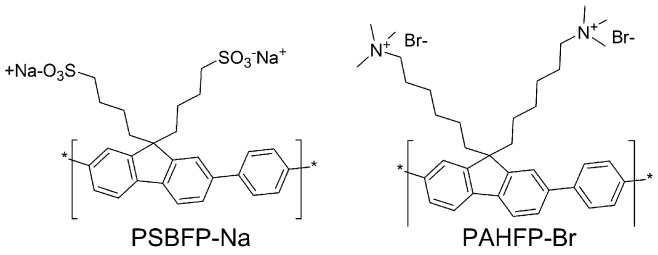

Figure 1. Molecular structures of the anionic (PSBFP-Na) and cationic (PAHFP-Br) CPEs.

Table 1. Device characteristics of PCDTBT:PC70BM OPVs with CPE interlayers. An external potential of 3 V was applied for 30 s for the electric poling process.

Cathode interlayer	V_{oc} [V]	J_{sc} [mA cm^{-2}]	FF [%]	PCE [%]	Resistance [Ω cm^2] R_{shunt}	R_{series}
no interlayer (Al only)	0.813	11.8	51.9	5	366	16.4
Ca	0.868	12.2	58.3	6.2	460.8	10.5
PSBFP-Na	0.894	12.1	63	6.8	493.2	7.9
PAHFP-Br	0.915	12	61.5	6.8	498.6	7

device with the anionic PAHFP-Na interlayer had a fill factor (FF) of 60.3%, an open-circuit voltage (V_{oc}) of 0.912 V, a short-circuit current density (J_{sc}) of 11.7 mA cm^{-2}, and a PCE of 6.6%. The device with the cationic PSBFP-Br interlayer had FF = 58%, V_{oc} = 0.905 V, J_{sc} = 12.3 mA cm^{-2}, and PCE = 6.5%, which shows substantial improvements in the device characteristics compared to that without a CPE (FF = 51.9%, V_{oc} = 0.813 V, J_{sc} = 11.8 mA cm^{-2}, PCE = 5.0%).

One proposed mechanism of WF modification in dipolar materials that include CPEs deposited on semiconductor or conductor substrate is that image charge attraction may cause an interfacial dipole to form between a dipole interlayer and a substrate.[27] In this mechanism, the image charges form the interfacial dipole; its magnitude and direction are determined by the differences in geometrical size and movability of the positive and negative parts. However, our PCDTBT:$PC_{70}BM$ device with the CPE interlayer showed a significantly improved PCE, irrespective of the ion polarity of PSBFP-Na and PAHFP-Br, if a metal electrode (Al) was deposited on the CPE layer. The

conventional models with regard to the mechanisms of dipole alignment (or spontaneous polarization) formation at the interface that include ultrathin CPE layers include hydrophilic and hydrophobic interactions at the interface and image charge attraction, which depends on the difference in the geometric size and movability of polar constituents in the CPE interlayer.[3–19,27] The identical effects of PAHFP-Na and PSBFP-Br interlayers as an electron extraction layer imply that these conventional models do not fully explain the mechanism by which the interfacial dipoles are generated and oriented.

On measuring the current–voltage (*J–V*) characteristics of the devices, we noticed that the device characteristics increased continuously as the number of voltage sweeps increased. On the basis of this interesting observation, we applied the external electric field to the device that included the CPE interlayer to a DC power supply, so-called electric poling. The *J–V* characteristics of the PCDTBT:$PC_{70}BM$ device that includes the CPE interlayer were obtained under the irradiation of air mass (AM)-1.5 global simulated sunlight at an intensity of 100 mW cm^{-2} (Figure 2). The PCDTBT:$PC_{70}BM$ device with

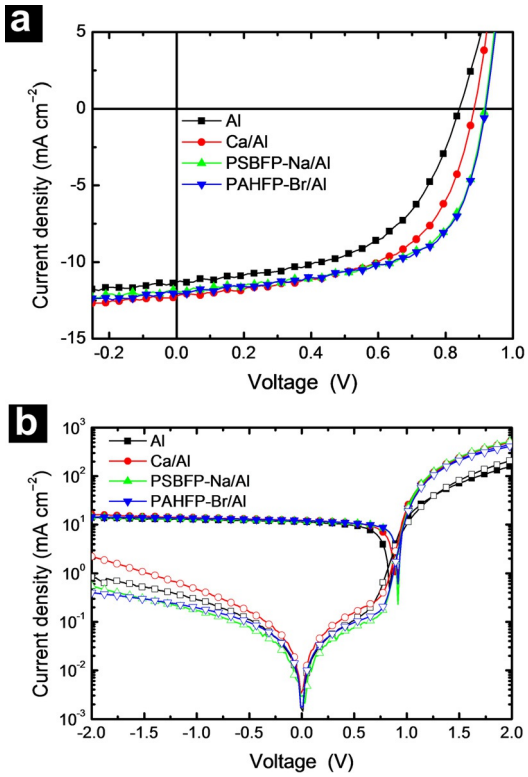

Figure 2. a) *J–V* curve of the electrically poled PCDTBT:$PC_{70}BM$ device with CPE interlayers at 100 mW cm^{-2}; b) log *J* vs. *V* under illumination (filled symbols) and in the dark (open symbols).

electrically poled CPE interlayers showed substantially higher V_{oc} and FF values than the device without the CPE interlayer. Therefore, the resulting PCE was improved to 6.8% after electric poling at 3 V for 30 s irrespective of the ionic groups of the CPEs (Table 1). The V_{oc} of the ITO/PEDOT:PSS/PCDTBT:$PC_{70}BM$/CPE/Al device is higher than that of the device without an interlayer or PCDTBT:$PC_{70}BM$/Ca/Al because the dipole moment of the CPEs induced a shift of the E_{vac} at the electrode interface and increased the built-in potential in the device (Figure 2a). The dark current of the PCDTBT:$PC_{70}BM$/CPE/Al devices was increased greatly compared with that of the PCDTBT:$PC_{70}BM$/Al devices; this difference implies that CPE/Al makes a better electron injection contact than Al alone. In addition, the rectification ratio (forward-biased current/reverse-biased current) at ±2.0 V in the dark *J–V* characteristic curve was ~10^3 for the device with 3 nm thick CPEs but ~10^2 for the device without the interlayer and with 3 nm thick Ca (Figure 2b).

Furthermore, we investigated the photovoltaic characteristics of ITO/PEDOT:PSS/PCDTBT:$PC_{70}BM$/PSBFP-Na/Al devices as a function of the poling electric field strength and poling time (Figure 3). The PCE and FF of the device increased gradually

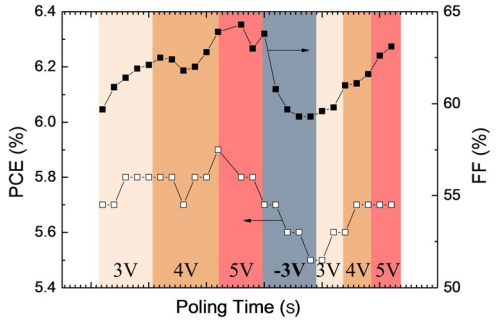

Figure 3. PCE and FF of the PCDTBT:$PC_{70}BM$ device with PSBFP-Na interlayer as a function of the applied poling potential and poling time.

with increasing poling time (5–40 s) and the poling potential (3–5 V, converted to 0.38–0.63 V μm^{-1} for a PCDTBT:$PC_{70}BM$/PSBFP-Na thickness of 83 nm). If we applied a reverse bias of −3 V to the device, the FF decreased drastically to an even lower value than that before poling. However, the FF recovered immediately if a positive bias was applied subsequently. Interestingly, the interfacial dipoles with the CPE interlayer were poled reversibly, which depended on the direction of the applied voltage.

We investigated the WF and the dipole moment of the ITO/PCDTBT:$PC_{70}BM$/CPE surface using Kelvin probe (KP) measurements. The WF of PSBFP-Br and PAHFP-Br interlayers on top of PCDTBT:$PC_{70}BM$ were 4.63 and 4.87 eV, which were, respectively, 0.15 eV lower and 0.07 eV higher than that of ITO/PCDTBT:$PC_{70}BM$ (Table 2). The PSBFP-Br and the PAHFP-Na

Table 2. KP measurement of the PCDTBT:PC70BM surface with a CPE interlayer. The WF of PCDTBT:$PC_{70}BM$/CPE was shifted oppositely depending on the CPE molecules. After positive electric poling, the WF value of both films was increased.

Interlayer on ITO/PCDTBT:$PC_{70}BM$	WF [eV]	
	before poling	after poling (+5 V 60 s)
ITO/PCDTBT:$PC_{70}BM$ (no interlayer)	4.78	4.76
ITO/PCDTBT:$PC_{70}BM$/PSBFP-Na	4.85	4.98
ITO/PCDTBT:$PC_{70}BM$/PAHFP-Br	4.63	4.90

layers showed the opposite dipole alignment on the PCDTBT:$PC_{70}BM$ layer because the most mobile counterions (Na^+ or Br^- in the CPE structures) tend to be located at the top near the air because of their intimate interaction with the surrounding polar solvent during the formation of the CPE thin film.

To investigate the distribution of ionic groups with the resulting dipole alignment after electric poling, we applied the forward bias through the metal foil electrode attached on the ITO/PCDTBT:$PC_{70}BM$/CPE surface and used the KP technique to measure the WF of the surface after detaching the foil electrode. The WF of both cationic and anionic CPE deposited films increased after the positive poling of 5 V for 60 s (Table 2). Schematics of the dipole moment formation at the interface of PCDTBT:$PC_{70}BM$/CPE explain the mechanism by which the direction of the dipole moment formed at the interfaces that include the PAHFP-Br layers was converted into an opposite direction that points toward PCDTBT:$PC_{70}BM$ layer by electric poling (Figure S1). Compared to the untreated ITO/PCDTBT:$PC_{70}BM$ film, the WF of the PAHFP-Br surface on the photoactive blend film (ITO/PCDTBT:$PC_{70}BM$/PAHFP-Br) was 0.15 eV lower before positive poling but 0.14 eV higher after positive poling. Both cationic and anionic CPE thin layers generate a surface dipole moment in the same direction at the interfaces even if PSBFP-Br has counterions charged oppositely to PAHFP-Na, in which the counterions are redistributed and orientated by the external electric field during electric poling. An energy level diagram of the PCDTBT:$PC_{70}BM$ solar cell using the CPE interlayer is summarized in Figure S2. In previous reports, ion redistribution models have been proposed to explain the possible mechanisms with regard to the change of dipole moment at the interface that includes CPE layers.[28,29]

The schematic ionic distribution and energy level diagram of the PAHFP-Br interlayer atop a photoactive layer are illustrated in Figure 4. The Br^- counterions of PAHFP-Br are located near the surface of the metal electrode and the polymer backbone that contains quaternary ammonium side chains is located close to the photoactive layer in the as-cast PAHFP-Br film (Figure 4a). Therefore, the interfacial dipole moment (μ_{ID}) points toward the metal surface before electrical poling. However, the Br^- ions and side chains that contain quaternary ammonium are forced to relocate under a positive electric field, so the μ_{ID} is altered to point toward the active layer (Figure 4b). As a result of the electrostatic force during positive electric poling, the anions (Br^- or $-SO_3^-$) can be redistributed toward the active layer surface and the cations (Na^+ or $-N(CH_3)_3^+$) can be redistributed toward the metal surface. The μ_{ID} values are determined primarily by the interfacial polarization that originates from the direct intimate contact of CPE with the metal or organic photoactive layer and not by the intrinsic molecular dipoles (μ_{MD}) of the bulk CPE layer. Similar results have been reported earlier that seem to contradict the predicted μ_{MD} alignment of the self-assembled monolayer (SAM).[30] If the dipolar molecules are directly in contact with the electrode, the metal–molecule contact at the interface makes the interfacial polarization possible. Therefore, the Schottky barrier at ZnO/SAM-X/Al (X = electron-donating group) decreased by the net dipole, which is identical to μ_{ID}, whereas the μ_{MD} of the SAM layer formed in the opposite direction to μ_{ID}. In our PCDTBT:$PC_{70}BM$/CPE/Al, the cationic $-N(CH_3)_3^+$ groups of PAHFP-Br are redistributed and located at the side of the Al surface after the positive electric poling, therefore, the E_{vac} shift is changed to the opposite direction to that before electric poling. The reason that the PCEs of the OPV devices with PSBFP-Br and PAHFP-Na interlayers were improved significantly irrespective of the ion functionality even before electric poling (compared with the PCE of the device without interlayers) is probably the simultaneous electric poling that occurred during *J–V* scans of the devices. However, this dipole reorientation was not completed during *J–V* measurement, so additional external electric poling can enhance the PCEs further.

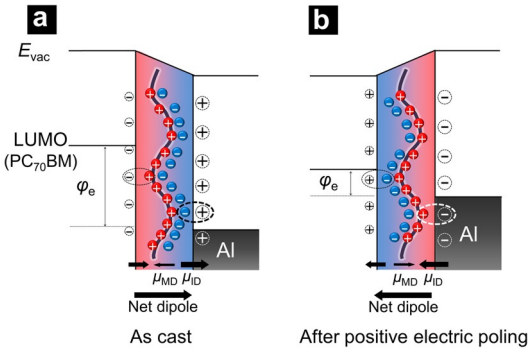

Figure 4. Schematic energy level diagrams of the PAHFP-Br interlayer on the photoactive layer surface. a) The introduction of PAHFP-Br interlayer results in vacuum level E_{vac} shift caused by the interfacial dipole μ_{ID} pointing toward the Al layer. b) After positive electric poling, the bromide counterions were redistributed and μ_{ID} points towards the active layer to decrease electron injection barrier (ϕ_e). Net dipoles are determined not by the intrinsic molecular dipole μ_{MD} of CPEs but by the μ_{ID} at the intimate contact interface.

If a metal electrode was not placed on top of the CPE layers, the distribution of the ionic groups in the CPE layer can be estimated roughly by analysis of the energy levels, such as the E_{vac} shift[14,16] or surface potential change,[4,22] by UV photoelectron spectroscopy and KP measurements. However, if the CPE layer is sandwiched between an organic photoactive layer and a metal film, the distribution of ionic moieties in the CPE film can be controlled systematically by applying the external electric field. Therefore, it is clear that the dipole moment and resulting WF changes at interfaces that include the CPE polar molecules come from the interfacial polarization that originates from the direct intimate contact of CPE with the metal or semiconducting photoactive layer. In addition, we compared the dipole moment change of CPEs on the hydrophobic photoactive layer with that on the hydrophilic ITO surface (Table S1). CPE layers (3 nm thick) were spin cast from isopropyl alcohol (IPA)/water and water solution for PSBFP-Na and PAHFP-Br, respectively. The effective WF of ITO/PAHFP-Na and ITO/PSBFP-Br were 0.13 eV higher and 0.17 eV lower than ITO substrate, respectively. Although UV O_3 treatment was conducted on the ITO surface, the directions of the dipole moment were not changed. The dipole direction of the ITO surface that includes a CPE layer was not changed upon electric poling unlike the CPE layer on PCDTBT:$PC_{70}BM$ (Table S1);

the difference can be attributed to stronger ion interaction and alignment of polar CPEs with the ITO surface than with the PCDTBT:$PC_{70}BM$. Interestingly, the ionic groups in the as-cast CPEs are distributed and organized to have the same dipole direction regardless of the substrates (hydrophilic ITO vs. hydrophobic photoactive layer) before electric poling. As ionic groups interact intimately with the surrounding polar solvent in dilute solution (0.1 wt% for PAHFP-Na, 0.05 wt% for PSBFP-Br), they might be located preferentially at the side of the air surface of the layer during spin coating.

As μ_{ID} reduced the electron injection barrier ϕ_e at the interface between the active layer and the metal (Figure 4), the introduction of electrically poled PSBFP-Na and PAHFP-Br interlayers can improve the device characteristics of OPVs. The E_{vac} shift of the CPEs interlayer caused a good alignment of the LUMO of $PC_{70}BM$ with WF of the Al electrode. Therefore, the performance parameters and PCE of the device were increased significantly by using the CPE interlayers and electric poling.

We investigated the *J–V* characteristics of the PCDTBT:$PC_{70}BM$ organic solar cells under different illumination intensities to understand the recombination process of the organic solar cells with CPEs (Figure S4). Nongeminate recombination was reduced in the device based on CPE/Al than that of the Al-only device because of the reduced energy level offset at the well-aligned contact in the device with CPE interlayers compared with the device with Al only (Figure S5). This is correlated with the observed increase of shunt resistance (R_{shunt}) and J_{sc} in the devices with CPEs (Table 1, Figure 2). In addition, electron transport in the space charge-limited current (SCLC) devices with and without CPEs was compared (Figures S6 and S7) and the corresponding electron mobilities of the devices were estimated (Table S2). The electron mobility and current density of the devices with CPEs were higher than that of devices with Al only. This is because of the lower energy level offset at the well-aligned contact in the device with CPE interlayers compared with that in the Al-only device.

We also used PTB7:$PC_{70}BM$ for a photoactive layer with the CPE interfacial layer and achieved a higher PCE with the electric poling process (Figure 5, Table 3). After electric poling for the devices with PAHFP-Na (+4 V) and PSBFP-Br (+5 V) interlayers, we achieved a PCE of 8.3% in both devices, which is higher than that of the PAHFP-Na (8.0%) and PSBFP-Br (7.7%) devices without electric poling. This difference demonstrates that the improvement of the photovoltaic properties in OPVs with PAHFP-Na and PSBFP-Br occurs irrespective of ion functionality in the normal OPV devices.

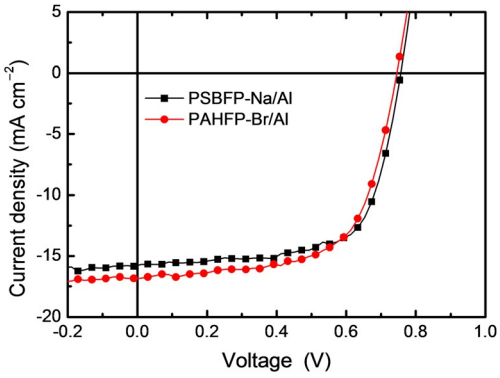

Figure 5. *J–V* curve of the electrically poled PTB7:$PC_{70}BM$ device with CPE interlayers at 100 mW cm^{-2}.

Table 3. Device characteristics of PTB7:$PC_{70}BM$ OPVs with CPE interlayers.

Cathode interlayer	V_{oc} [V]	J_{sc} [mA cm^{-2}]	FF [%]	PCE [%]
no interlayer (Al only)	0.77	13	62.2	6.2
PSBFP-Na	0.766	15.9	68	8.3
PAHFP-Br	0.749	17	64.9	8.3

Conclusions

We demonstrated that the mechanism by which the interfacial dipoles of conjugated polyelectrolytes (CPEs) are generated and oriented at cathode interlayers and, in contrast to the conventional understanding, the power conversion efficiency (PCE) can be improved significantly by both cationic and anionic CPE interlayers regardless of the ion functionality (i.e., cationic or anionic) of the CPE. Through the application of an external bias to devices (so-called electric poling), the ionic groups in the CPE layer were redistributed and the interfacial dipoles (μ_{ID}) were realigned to improve the energy level alignment at the interface between the photoactive layer and the electrode. In addition, the energy level alignment and the performance parameter of organic photovoltaics (OPVs) with CPE interlayers were controlled systematically by adjusting the electric field strength and the duration of electric poling. The energy level adjustment of the CPE interlayer was determined not by the intrinsic molecular dipole (μ_{MD}) of the bulk CPE layer but by the μ_{ID}, which originates from the direct intimate contact of CPE with the metal or organic photoactive layer. Finally we obtained a high PCE in the poly({4,8-bis[(2-ethylhexyl)oxy]benzo[1,2-b:4,5-b′]dithiophene-2,6-diyl}{3-fluoro-2-[(2-ethylhexyl)-carbonyl] thieno[3,4-b]thiophenediyl}):[6,6]-phenyl C70-butyric acid methyl ester/CPE devices (8.3%) because the CPE interlayers reduce the electron injection barrier and thereby increase the performance parameters after electric poling.

Experimental Section

Synthesis and characterization of CPEs (PSBFP-Na and PAHFP-Br)

The conjugated polyelectrolyte CPE was synthesized by a modification of procedures reported previously.[8] PSBFP-Na was synthesized by the Suzuki polymerization of 2,7-dibromo-9,9-bis(4-sulfonatobutyl)fluorene disodium[31] and 1,4-phenylenebisboronic ester using $Pd(OAc)_2$ in DMF/pH 10 buffer (1:2 by volume) at 80 °C for 24 h. The anionic polymer was purified by dialysis by using a 12400 g mol^{-1} cut-off membrane and obtained by freezing drying. ^{1}H NMR (300 MHz, [D_6]DMSO): δ = 7.90–7.34 (br, 10H), 2.31–2.15 (m, 4H), 2.10–2.02 (m, 4H), 1.42–1.36 (m, 4H), 0.63–0.60 ppm (m, 4H).

PAHFP-Br was prepared by Suzuki polymerization and a successive quaternization reaction. The neutral precursor, poly[9,9′-bis(6′′-bromohexyl)fluorene-*co-alt*-1,4-phenylene][32] was synthesized by the Suzuki coupling of 2,7-dibromo-9,9-bis(6-bromohexyl)fluorene[33] and 1,4-phenylenebisboronic ester with $Pd(PPh_3)_4$ in toluene/K_2CO_3 (2 M in water; 2:11 by volume) at 80 °C for 24 h. The cationic CPE was obtained by treating the neutral polymer with a 30% aqueous solution of trimethylamine in THF/methanol for 48 h. ^{1}H NMR (300 MHz, DMSO): $\delta = 8.10–7.60$ (br, 10H), 3.17 (br, 4H), 2.96 (s, 18H), 1.6–0.9 ppm (br, 20H).

Device fabrication

A PEDOT:PSS (CLEVIOS PH) dispersion was diluted in IPA (1:1 *w/w*), spin-coated to give a 35 nm thick hole extraction layer on top of ITO/glass, and baked on a hotplate in air at 200 °C for 10 min. The blend of PCDTBT (1-material; 7 mg) and $PC_{70}BM$ (from Nano-C Inc.; 28 mg) in 1,2-dichlorebenzene (DCB; 1 mL) was prepared for the photoactive layer. PCDTBT:$PC_{70}BM$ layers were spin-coated at 1600 rpm for 60 s to make 80 nm thick films and then annealed thermally at 70 °C for 10 min in a N_2-filled glovebox. For the device with a CPE as an interlayer, a PSBFP-Na or PAHFP-Br solution dissolved in distilled water or IPA/distilled water (1:1 *v/v*), respectively, was deposited by spin-coating and dried at 60 °C for 10 min. The thickness of the CPE was controlled by solution concentration and spin-coating conditions. The average thickness was measured by ellipsometry as 3 nm at 2000 rpm with 0.05 wt% solution for PAHFP-Br and 0.1 wt% solution for PSBFP-Na. The Ca interlayer was evaporated thermally on the photoactive layer at a deposition rate of 0.2 Å s^{-1} under a high vacuum ($< 5\times10^{-7}$ Torr), and the Al cathode was deposited sequentially: first, 20 nm thickness at a deposition rate of 1 Å s^{-1} and then 80 nm thickness at 3 Å s^{-1} under high vacuum ($< 5\times10^{-7}$ Torr). The photoactive area (0.06 cm^2) was defined by using metallic shadow masks. The devices were encapsulated with a glass lid by using a UV-curable epoxy resin in a N_2-filled glovebox.

Device characterization

The *J–V* characteristics were obtained by using a computer-controlled Keithley 2400 source measurement unit under simulated solar AM 1.5G illumination (100 mW cm^{-2}) generated by using a solar simulator system based on a xenon lamp (Newport 69907, Class AAA, 450 W).

KP measurement

WF values for ITO/CPE and ITO/PCDTBT:$PC_{70}BM$/CPE were measured by using a SKP5050 Scanning Kelvin Probe (KP Technology Ltd.) with a gold probe with a diameter of 2 mm.

Acknowledgements

This work was supported by the Center for Advanced Soft-Electronics funded by the Ministry of Science, ICT and Future Planning as Global Frontier Project (2014M3A6A5060947). This work was also supported by the National Research Foundation (NRF) of Korea (2012M3A6A7055540).

Keywords: electrolytes · electron transport · interfaces · photovoltaics · polymers

[1] a) M. O. Reese, M. S. White, G. Rumbles, D. S. Ginley, S. E. Shaheen, *Appl. Phys. Lett.* **2008**, *92*, 053307; b) V. D. Mihailetchi, P. W. M. Blom, J. C. Hummelen, M. T. Rispens, *J. Appl. Phys.* **2003**, *94*, 6849; c) X. Jiang, H. Xu, L. Yang, M. Shi, M. Wang, H. Chen, *Sol. Energy Mater. Sol. Cells* **2009**, *93*, 650; d) S. K. M. Jönsson, E. Carlegrim, F. Zhang, W. R. Salanck, M. Fahlman, *Jpn. J. Appl. Phys.* **2005**, *44*, 3695; e) C. J. Brabec, S. E. Shaheen, C. Winder, N. S. Sariciftci, *Appl. Phys. Lett.* **2002**, *80*, 1288; f) L.-M. Chen, Z. Xu, Z. Hong, Y. Yang, *J. Mater. Chem.* **2010**, *20*, 2575; g) T.-W. Lee, K.-G. Lim, D.-H. Kim, *Electron. Mater. Lett.* **2010**, *6*, 41; h) J. H. Park, T.-W. Lee, B.-D. Chin, D. H. Wang, O. O. Park, *Macromol. Rapid Commun.* **2010**, *31*, 2095; i) H.-L. Yip, A. K.-Y. Jen, *Energy Environ. Sci.* **2012**, *5*, 5994; j) M.-R. Choi, T.-H. Han, K.-G. Lim, S.-H. Woo, D. H. Huh, T.-W. Lee, *Angew. Chem. Int. Ed.* **2011**, *50*, 6274; *Angew. Chem.* **2011**, *123*, 6398; k) K.-G. Lim, M.-R. Choi, H.-B. Kim, J. H. Park, T.-W. Lee, *J. Mater. Chem.* **2012**, *22*, 25148; l) K.-G. Lim, M.-R. Choi, J. H. Kim, D. H. Kim, G. H. Jung, Y. Park, J. L. Lee, T.-W. Lee, *ChemSusChem* **2014**, *7*, 1125; m) S. Kwon, K.-G. Lim, M. Shim, H. C. Moon, J. Park, G. Jeon, J. Shin, K. Cho, T.-W. Lee, J. K. Kim, *J. Mater. Chem. A* **2013**, *1*, 11802; n) K.-G. Lim, H.-B. Kim, J. Jeong, H. Kim, J. Y. Kim, T.-W. Lee, *Adv. Mater.* **2014**, *26*, 6461.

[2] Z. C. He, C. Zhang, X. F. Xu, L. J. Zhang, L. Huang, J. W. Chen, H. B. Wu, Y. Cao, *Adv. Mater.* **2011**, *23*, 3086.

[3] Z. He, C. Zhong, S. Su, M. Xu, H. Wu, Y. Cao, *Nat. Photonics* **2012**, *6*, 591.

[4] Z. He, C. Zhong, X. Huang, W. Y. Wong, H. Wu, L. Chen, S. Su, Y. Cao, *Adv. Mater.* **2011**, *23*, 4636.

[5] L. Chen, C. Xie, Y. Chen, *Org. Electron.* **2013**, *14*, 1551.

[6] C. He, C. Zhong, H. B. Wu, R. Yang, W. Yang, F. Huang, G. C. Bazan, Y. Cao, *J. Mater. Chem.* **2010**, *20*, 2617.

[7] J. Luo, H. B. Wu, C. He, A. Y. Li, W. Yang, Y. Cao, *Appl. Phys. Lett.* **2009**, *95*, 043301.

[8] T. Yang, M. Wang, C. Duan, X. Hu, L. Huang, J. Peng, F. Huang, X. Gong, *Energy Environ. Sci.* **2012**, *5*, 8208.

[9] T.-W. Lee, O. O. Park, *Adv. Mater.* **2001**, *13*, 1274.

[10] J. Yoon, J. J. Kim, T.-W. Lee, O. O. Park, *Appl. Phys. Lett.* **2000**, *76*, 2152.

[11] T.-W. Lee, O. O. Park, L.-M. Do, T. Zyung, T. Ahn, H.-K. Shim, *J. Appl. Phys.* **2001**, *90*, 2128.

[12] B. H. Lee, I. H. Jung, H. Y. Woo, H.-K. Shim, G. Kim, K. Lee, *Adv. Funct. Mater.* **2014**, *24*, 1100.

[13] S. H. Oh, S. I. Na, J. Jo, B. Lim, D. Vak, D. Y. Kim, *Adv. Funct. Mater.* **2010**, *20*, 1977.

[14] R. Kang, S.-H. Oh, D.-Y. Kim, *ACS Appl. Mater. Interfaces* **2014**, *6*, 6227.

[15] S.-I. Na, T.-S. Kim, S.-H. Oh, J. Kim, S.-S. Kim, D.-Y. Kim, *Appl. Phys. Lett.* **2010**, *97*, 223305.

[16] J. H. Seo, T.-Q. Nguyen, *J. Am. Chem. Soc.* **2008**, *130*, 10042.

[17] H. Choi, J. S. Park, E. Jeong, G.-H. Kim, B. R. Lee, S. O. Kim, M. H. Song, H. Y. Woo, J. Y. Kim, *Adv. Mater.* **2011**, *23*, 2759.

[18] W. Lee, H. Choi, S. Hwang, J. Y. Kim, H. Y. Woo, *Chem. Eur. J.* **2012**, *18*, 2551.

[19] J. Jo, J.-R. Pouliot, D. Wynands, S. D. Collins, J. Y. Kim, T. L. Nguyen, H. Y. Woo, Y. Sun, M. Leclerc, A. J. Heeger, *Adv. Mater.* **2013**, *25*, 4783.

[20] K. Yao, L. Chen, Y. Chen, F. Li, P. Wang, *J. Mater. Chem.* **2011**, *21*, 13780.

[21] J. Seo, A. Gutacker, Y. M. Sun, H. B. Wu, F. Huang, Y. Cao, U. Scherf, A. J. Heeger, G. C. Bazan, *J. Am. Chem. Soc.* **2011**, *133*, 8416.

[22] L. Chen, C. Xie, Y. Chen, *Macromolecules* **2014**, *47*, 1623.

[23] S. H. Park, A. Roy, S. Beaupre, S. Cho, N. Coates, J. S. Moon, D. Moses, M. Lederc, K. Lee, A. J. Heeger, *Nat. Photonics* **2009**, *3*, 297.

[24] N. Blouin, A. Michaud, M. Leclerc, *Adv. Mater.* **2007**, *19*, 2295.

[25] H. Yi, S. Al-Faifi, A. Iraqi, D. C. Watters, J. Kingsley, D. G. Lidzey, *J. Mater. Chem.* **2011**, *21*, 13649.

[26] D.-H. Kim, K.-G. Lim, J. H. Park, T.-W. Lee, *ChemSusChem* **2012**, *5*, 2053.

[27] S. van Reenen, S. Kouijzer, R. A. J. Janssen, M. M. Wienk, M. Kemerink, *Adv. Mater. Interfaces* **2014**, *1*, 1400189.

[28] a) C. Hoven, R. Yang, A. Garcia, A. J. Heeger, T.-Q. Nguyen, G. C. Bazan, *J. Am. Chem. Soc.* **2007**, *129*, 10976; b) R. Yang, A. Garcia, D. Korystov, A. Mikhailovsky, G. C. Bazan, T.-Q. Nguyen, *J. Am. Chem. Soc.* **2006**, *128*, 16532; c) A. Garcia, R. C. Bakus II, P. Zalar, C. V. Hoven, J. Z. Brzezinski, T.-

Q. Nguyen, *J. Am. Chem. Soc.* **2011**, *133*, 2492; d) C. V. Hoven, A. Garcia, G. C. Bazan, T. Q. Nquyen, *Adv. Mater.* **2008**, *20*, 3793.
[29] J. Fang, B. H. Wallikewitz, F. Gao, G. Tu, C. Müller, G. Pace, R. H. Friend, W. T. S. Huck, *J. Am. Chem. Soc.* **2011**, *133*, 683.
[30] H. L. Yip, S. K. Hau, N. S. Baek, H. Ma, A. K. Y. Jen, *Adv. Mater.* **2008**, *20*, 2376.
[31] K.-Y. Pu, K. Li, B. Liu, *Chem. Mater.* **2010**, *22*, 6736.
[32] R. Mallavia, F. Montilla, I. Pastor, P. Velásquez, B. Arredondo, A. L. Álvarez, C. R. Mateo, *Macromolecules* **2005**, *38*, 3185.
[33] M. Stork, B. S. Gaylord, A. J. Heeger, G. C. Bazan, *Adv. Mater.* **2002**, *14*, 361.

Received: May 9, 2015
Revised: July 7, 2015
Published online on September 8, 2015